Tip-Based Hybrid Simulation Study of Frictional Properties of Self-Assembled Monolayers: Effects of Chain Length, Terminal Group, Scan Direction, and Scan Velocity

ARTICLE *in* LANGMUIR · NOVEMBER 2003

Impact Factor: 4.46 · DOI: 10.1021/la034007g

3 AUTHORS, INCLUDING:

Luzheng Zhang
xF Technologies
47 PUBLICATIONS **967** CITATIONS
SEE PROFILE

Yongsheng Leng
George Washington University
56 PUBLICATIONS **767** CITATIONS
SEE PROFILE

Tip-Based Hybrid Simulation Study of Frictional Properties of Self-Assembled Monolayers: Effects of Chain Length, Terminal Group, Scan Direction, and Scan Velocity

Luzheng Zhang,† Yongsheng Leng,‡ and Shaoyi Jiang*

Department of Chemical Engineering, University of Washington, Seattle, Washington 98195

Received January 3, 2003. In Final Form: August 14, 2003

We report a study of the frictional properties of alkanethiol self-assembled monolayers (SAMs) on Au(111) at room temperature using hybrid molecular simulations at the atomic force/frictional force microscopy (AFM/FFM) experimental time scale. Various parameters influencing frictional properties were investigated, including chain length, terminal group, scan direction, and scan velocity. Simulation results show that frictional force decreases with an increase of chain length and that hydrophilic −OH-terminated SAMs have higher frictional force than hydrophobic $-CH_3$-terminated SAMs. Frictional force as a function of normal load exhibits different behaviors for $-CH_3$- and −OH-terminated SAMs. Simulation results further show friction anisotropy on SAMs at low and high temperatures. Frictional force is the smallest when scanned along the tilt direction, the largest when scanned against the tilt direction, and between when scanned perpendicular to the tilt direction. Finally, simulation results also show the dependence of friction on scan velocity. Friction exhibits a maximum for hydrophobic $-CH_3$-terminated SAMs and decreases for hydrophilic −OH-terminated SAMs as scan velocity increases. It approaches a constant value at high scan velocities for both surfaces.

1. Introduction

Friction and adhesion are crucial factors that control the efficiency and durability of moving mechanical assemblies in micro- or nano-electromechanical systems (MEMS/NEMS).[1−3] These properties must be minimized for successful operation of MEMS/NEMS devices. Self-assembled monolayers (SAMs) are one of the strategies used for minimizing stiction and reducing adhesion and friction in those devices. Consequently, there has been considerable interest in investigating the frictional and adhesion properties of these SAMs. Atomic force/frictional force microscopy (AFM/FFM) is an ideal instrument to study the phenomena down to the atomic scale.[4] Furthermore, it allows the accurate measurements of forces applied in the horizontal as well as normal directions to a surface. It has been observed that the frictional force of alkanethiols on Au(111) decreases as the chain length of thiols increases from C_8 to C_{18}[5−7] or as the size of terminal groups decreases from $-CF_3$ to $-CH_3$[8,9] and that frictional force depends on scan direction,[10−12] scan velocity,[13−17] and environmental conditions (e.g., humidity).[18−20] AFM/FFM has also been applied to study the frictional properties of alkanethiol on Au with chemically modified tips (chemical force microscopy, CFM),[17,21−23] silanes,[24−27] and many other systems.[14,15,28−31]

To obtain a fundamental understanding of friction and adhesion at the molecular level, molecular dynamics (MD)

* To whom correspondence should be addressed. Phone: (206) 616-6509. Fax: (206) 685-3451. E-mail: sjiang@u.washington.edu.

† Current address: Materials and Process Simulation Center, 139-74, California Institute of Technology, Pasadena, CA 91125.

‡ Current addresses: Department of Chemical Engineering, Vanderbilt University, Nashville, TN 37235-1604, and Chemical Sciences Division, Oak Ridge National Laboratory, Oak Ridge, TN 37831-6110.

(1) (a) Maboudian, R.; Ashurst, W. R.; Carraro, C. *Tribol. Lett.* **2002**, *12*, 95. (b) Maboudian, R. *Surf. Sci. Rep.* **1998**, *30*, 207. (c) Maboudian, R.; Howe, R. T. *J. Vac. Sci. Technol., B* **1997**, *15*, 1.

(2) Maboudian, R.; Ashurst, W. R.; Carraro, C. *Sens. Actuators* **2000**, *82*, 219.

(3) Jiely, J. D.; Houston, J. E.; Mulder, J. A.; Hsung, R. P.; Zhu, X. Y. *Tribol. Lett.* **1999**, *7*, 103.

(4) Bonnell, D. A. *Scanning Probe Microscopy and Spectroscopy: Theory, Techniques, and Applications*, 2nd ed.; Wiley-VCH: New York, 2001.

(5) Li, L.; Yu, Q.; Jiang, S. *J. Phys. Chem. B* **1999**, *103*, 8290.

(6) Lio, A.; Charych, D. H.; Salmeron, M. *J. Phys. Chem. B* **1997**, *101*, 3800.

(7) McDermott, M. T.; Green, J.-B. D.; Porter, M. D. *Langmuir* **1997**, *13*, 2504.

(8) Kim, H. I.; Koini, T.; Lee, T. R.; Perry, S. S. *Langmuir* **1997**, *13*, 7192.

(9) Kim, H. I.; Graupe, M.; Oloba, O.; Koini, T.; Imaduddin, S.; Lee, T. R.; Perry, S. S. *Langmuir* **1999**, *15*, 3179.

(10) Overney, R. M.; Takano, H.; Fujihira, M.; Paulus, W.; Ringsdorf, H. *Phys. Rev. Lett.* **1994**, *72*, 3546.

(11) Hisada, K.; Knobler, C. M. *Langmuir* **2000**, *16*, 9390.

(12) Ohzono, T.; Fujihira, M. *Tribol. Lett.* **2000**, *9*, 63.

(13) Tsukruk, V. V.; Everson, M. P.; Lander, L. M.; Brittain, W. J. *Langmuir* **1996**, *12*, 3905.

(14) Bliznyuk, V. N.; Everson, M. P.; Tsukruk, V. V. *J. Tribol.* **1998**, *120*, 489.

(15) van der Vegte, E. W.; Subbotin, A.; Hadziioannou, G.; Ashton, P. R.; Preece, J. A. *Langmuir* **2000**, *16*, 3249.

(16) Liu, Y.; Evans, D. F.; Song, Q.; Grainger, D. W. *Langmuir* **1996**, *12*, 1235.

(17) Brewer, N. J.; Beake, B. D.; Leggett, G. J. *Langmuir* **2001**, *17*, 1970.

(18) Li, L.; Chen, S.; Jiang, S. *ACS Symposium Series*; Frommer, J. E., Overney, R., Eds.; American Chemical Society: Washington, DC, 2001; p 168.

(19) Tian, F.; Xiao, X.; Loy, M. M. T.; Wang, C.; Bai, C. *Langmuir* **1999**, *15*, 244.

(20) Zhang, L.; Li, L.; Chen, S.; Jiang, S. *Langmuir* **2002**, *18*, 5448.

(21) (a) Frisbie, C. D.; Tozsnyai, L. F.; Noy, A.; Wrighton, M. S.; Lieber, C. M. *Science* **1994**, *265*, 2071. (b) Noy, A.; Frisbie, C. D.; Rozsnyai, L. F.; Wrighton, M. S.; Lieber, C. M. *J. Am. Chem. Soc.* **1995**, *117*, 7943.

(22) Green, J.-B. D.; McDermott, M. T.; Porter, M. D.; Siperko, L. M. *J. Phys. Chem.* **1995**, *99*, 10960.

(23) Fujihira, M.; Tani, Y.; Furugoti, M.; Akiba, U.; Okabe, Y. *Ultramicroscopy* **2001**, *86*, 63.

(24) Fritz, M. C.; Carraro, C.; Maboudian, R. *Tribol. Lett.* **2001**, *11*, 171.

(25) Liu, Y.; Wu, T.; Evans, D. F. *Langmuir* **1994**, *10*, 2241.

(26) Clear, S. C.; Nealey, P. F. *J. Colloid Interface Sci.* **1999**, *213*, 238.

(27) Moser, A.; Eckhardt, C. J. *Thin Solid Films* **2001**, *382*, 202.

(28) Beake, B. D.; Leggett, G. J. *Langmuir* **2000**, *16*, 735.

(29) Li, J.; Wang, C.; Shang, G.; Xu, Q.; Lin, Z.; Guan, J.; Bai, C. *Langmuir* **1999**, *15*, 7662.

(30) Harrison, J. A.; White, C. T.; Colton, R. J.; Brenner, D. W. *Thin Solid Films* **1995**, *260*, 205.

(31) Qi, Y.; Cheng, Y. T.; Cagin, T.; Goddard, W. A., III. *Phys. Rev. B* **2002**, *66*, 085420.

10.1021/la034007g CCC: $25.00
Published on Web 10/09/2003

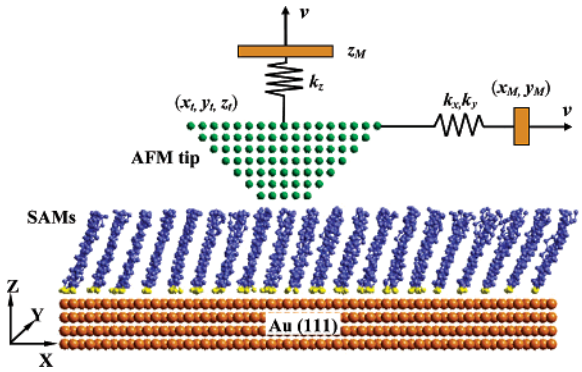

Figure 1. Schematic representation of the simulation system: AFM tip/cantilever assembly and alkanethiol SAMs on Au(111).

simulations have been performed to investigate the indentation and frictional properties of various organic monolayers, including SAMs[32−36] and the rupture of adhesive films bonded to solid substrates.[37] However, the difference in time scale between conventional MD simulations and AFM/FFM experiments is 6 orders of magnitude or larger. For example, the tip scan velocity in AFM/FFM experiments is ~400 nm/s, while it is in the order of m/s in conventional MD simulations. In addition, contact mechanics and detailed molecular information near the contact area in AFM/FFM have not been fully understood yet. Recently, we developed a temporally hybrid simulation technique to simulate adhesion and friction between $-CH_3$-terminated alkanethiol SAMs and a tip[38−40] at the AFM/FFM experimental time scale and found a chain-length dependence of friction for $-CH_3$-terminated alkanethiol SAMs on Au(111).[38] However, these simulations were performed at a lower temperature of 0.1 K. This hybrid simulation technique was recently extended to simulate adhesion and friction between SAM modified AFM tips and SAM surfaces at the CFM experimental time scale.[41] Two contact pairs, hydrophobic methyl/methyl ($-CH_3/-CH_3$) and hydrophilic hydroxyl/hydroxyl ($-OH/-OH$) terminated SAMs under dry lubrication conditions were studied. Results are in agreement with those from CFM experiments. In this work, we focus on how the frictional properties of $-CH_3$- and $-OH$-terminated alkanethiol SAMs on Au(111) vary with such parameters as chain length, terminal groups, scan direction, and scan velocity at room temperature. Results will be compared with those from AFM/FFM experiments.

2. Simulation Method

2.1. Hybrid Method. We recently developed a temporally hybrid molecular simulation technique,[38−40] in which a dynamic element model for the AFM/FFM cantilever is combined with a molecular dynamics relaxation approach for the rest of the system. Figure 1 shows the mechanical model of the simulation system. In simulations of adhesion, the AFM/FFM tip is dragged by the vertical support (z_M) through the spring (k_z) at a velocity of v, while the lateral support (x_M, y_M) is fixed. In simulations of lateral friction, the AFM/FFM tip is dragged by the lateral support (x_M, y_M) with constant y_M through the spring (k_x) at a velocity of v, where $x_M = vt$ and v is the scan velocity. In constant-load mode, the differential equations of motion of the AFM/FFM cantilever are governed by

$$M\ddot{x}_t = k_x(vt - x_t) - 2\gamma\sqrt{k_x M}\dot{x}_t + W_x(x_t,y_t,z_t; X(t)) \quad (1)$$

$$M\ddot{y}_t = k_y(y_M - y_t) - 2\gamma\sqrt{k_y M}\dot{y}_t + W_y(x_t,y_t,z_t; X(t)) \quad (2)$$

$$M\ddot{z}_t = F_{ext} + W_z(x_t,y_t,z_t; X(t)) \quad (3)$$

where the surface forces in the x, y, and z directions are denoted by W_x, W_y, and W_z, which depend not only on tip position (x_t, y_t, z_t), but also on the atomic substrate molecular configuration, including SAMs, $X(t)$ at time t. The damping γ is used to stabilize the motion of the tip,[40] and F_{ext} is the external applied load. Frictional force measured in the scan direction, F_x, is the first term on the right-hand side of eq 1, i.e., $F_x = k_x(vt - x_t)$.

The model system in this work is a rigid gold tip supported by an AFM/FFM cantilever in contact with alkanethiol SAMs chemisorbed onto a static Au(111) surface, which consists of 2400 Au atoms in four layers and has a size of (8.66 nm × 5.00 nm) in the $x-y$ plane (Figure 1). The tip is represented by a rigid pyramid exposing (001) facet and contains 280 Au atoms in seven layers. The bottom layer of the pyramidal tip is composed of nine Au atoms, corresponding to an effective contact area of 0.75 nm^2. The total number of SAMs chains in the model is 200, forming the basic $(\sqrt{3} \times \sqrt{3})R30°$ structure. The SAMs have a chain length of C_8, C_{12}, and C_{15} and are terminated with either hydrophobic $-CH_3$ (denoted as C_7CH_3, $C_{11}CH_3$, $C_{14}CH_3$, respectively) or hydrophilic $-OH$ (denoted as C_7OH, $C_{11}OH$, $C_{14}OH$, respectively) groups. Parameters used in simulations are from AFM/FFM experiments: the effective mass of the CFM tip $M = 10^{-11}$ kg; spring constants $k_x = 132$ N/m; $k_y = 100$ N/m; $k_z = 0.5$ N/m; scan velocity $v = 400$ nm/s.[5] These parameters are taken from AFM/FFM experiments and also have been used in our previous simulation studies.[38−40] To study the effect of scan velocity on friction, scan velocity was varied in a range of 100 nm/s−20 μm/s. All simulations were carried out at 300 K.

The basic idea of this hybrid simulation technique is that when the difference of the resonant frequencies between the cantilever and the molecular chain system is quite large, their energy modes can be decoupled. Integration of the dynamic equations of motion of the AFM/FFM cantilever and the molecular chain system can proceed separately, i.e., the macroscopic dynamic equations of motion of the cantilever is integrated with comparably larger time steps (μs) and then a fast relaxation of the atomic SAM surface/substrate with small time steps (fs) is followed. In this work, the equations of motion for the tip were integrated over $100\Delta t_{tip}$, where time step Δt_{tip} equals 0.5 μs (equivalent to the displacement of the support by 0.02 nm at $v = 400$ nm/s) using a backward differation (BD) algorithm. Then, the SAM atoms (S, CH_2, CH_3) were relaxed over $500\Delta t_{MD}$ using the velocity Verlet algorithm with bond constraints (RATTLE)[42] with a MD time step $\Delta t_{MD} = 1.0$ fs. Hybrid simulations were performed previously at lower temperature (0.1 K).[38−40] Results from our recent hybrid simulations at 300 K[41] showed that MD relaxation over 300, 600, and $1200\Delta t_{MD}$ yielded the same force−distance curve, indicating that the relaxation of SAMs is quite fast. In this work, $500\Delta t_{MD}$ was used for SAM relaxation at 300 K.

2.2. Potential Model and Simulation Details. The simulation system includes alkanethiol chains, substrate, and tip consisting of Au atoms. Interaction potentials for this system were described in details previously.[35,38−41] The united atom (UA) model[43] with bond constraints was adopted to describe the structure of alkanethiol SAMs/Au(111).[41,44,45] The total potential energy is represented by a superposition of valence and nonbond interactions. The valence terms consist of bond stretch, bond-

(32) Glosli, J. N.; McClelland, G. M. *Phys. Rev. Lett.* **1993**, *70*, 1960.
(33) (a) Tupper, K. J.; Colton, R. J.; Brenner, D. W. *Langmuir* **1994**, *10*, 2041. (b) Tupper, K. J.; Brenner, D. W. *Thin Solid Films* **1994**, *253*, 185.
(34) (a) Mikulski, P. T.; Harrison, J. A. *J. Am. Chem. Soc.* **2001**, *123*, 6873. (b) Mikulski, P. T.; Harrison, J. A. *Tribol. Lett.* **2001**, *10*, 29.
(35) Zhang, L.; Jiang, S. *J. Chem. Phys.* **2002**, *117*, 1804.
(36) Chandross, M.; Grest, G. S.; Stevens, M. J. *Langmuir* **2002**, *18*, 8392.
(37) Baljon, A. R. C.; Robbins, M. O. *Science* **1996**, *271*, 482.
(38) Leng, Y. S.; Jiang, S. *J. Chem. Phys.* **2000**, *113*, 8800.
(39) Leng, Y. S.; Jiang, S. *Phys. Rev. B* **2001**, *63*, 193406.
(40) Leng, Y. S.; Jiang, S. *Tribol. Lett.* **2001**, *11*, 111.
(41) Leng, Y. S.; Jiang, S. *J. Am. Chem. Soc.* **2002**, *124*, 11764.
(42) Allen M. P.; Tildesley, D. J. *Computer simulation of liquids*; Oxford: New York, 1987.
(43) Ryckaert, J.; Bellemans, A. *Discuss. Faraday Soc.* **1978**, *66*, 95.
(44) Zhang, Q.; Zheng, J.; Shevade, A. V.; Zhang, L.; Gehrke, S. H.; Hefflefinger, G. S.; Jiang, S. *J. Chem. Phys.* **2002**, *117*, 808.
(45) Hautman, J.; Klein, M. L. *J. Chem. Phys.* **1989**, *91*, 4994.

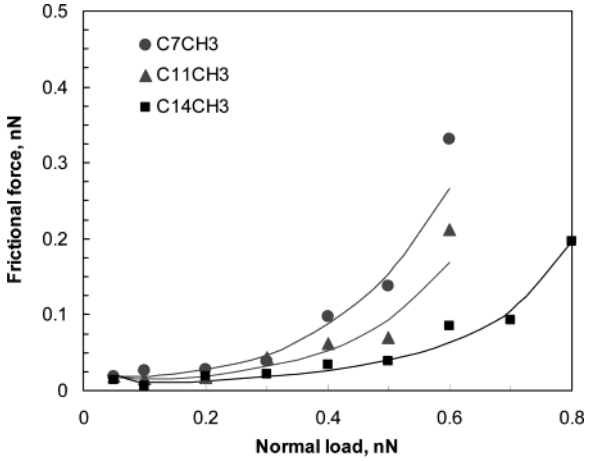

Figure 2. Frictional force vs normal load for $-CH_3$-terminated alkanethiol SAMs of different chain lengths at $v = 400$ nm/s, $T = 300$ K, and $\theta = 0°$. Lines are drawn to guide the eyes.

angle bending, and dihedral angle torsion terms, while the nonbond interactions consist of van der Waals (vdw) and electrostatic terms. The nonbonded interactions are not used between nearest neighbors (1−2 interactions) and between next-nearest neighbors (1−3 interactions). The vdw term takes into account both intermolecular and intramolecular interactions. For alkanethiol chains terminated with $-CH_3$ no Columbic interaction was taken into account, while, for those terminated with −OH, the optimized potential for liquid simulations (OPLS) was used.[46] Only the last three interaction sites in the terminal groups were assumed to have charges. All force field parameters (inter- and intramolecular interactions) for Au substrate atoms and molecular chains (S, CH_2, and CH_3) were given elsewhere.[38−41] The Columbic interactions between charged interaction sites were truncated at a distance of 25 Å.

The initial configurations of simulations were set up and minimized by the commercial software, CERIUS2.[47] In all MD simulations, alkanethiol molecules were dynamic, while substrate and tip Au atoms were fixed. It has been shown that dynamics of wall atoms has no significant influence on friction properties.[35] Temperature was kept constant by rescaling the velocities at every 10 time steps. The 20 000-step MD simulations were performed before the production run, for which 50 000-step MD simulations (equivalent to the tip scanned at a total distance of 20 Å) were then carried out for friction studies.

3. Results and Discussion

3.1. Chain-Length Dependence. In simulations of friction, the scan velocity of the support in eq 1 was set to 400 nm/s. We assume that the spring constant in the *y* direction is sufficiently large to prevent two-dimension scanning of the tip. In this work, all simulations were carried out with a spring constant k_x of 132 N/m (hard spring). The frictional force was obtained by averaging instant frictional force over scanning distance.[38−41] An error of ∼10% in the mean frictional force was obtained when the tip scanned across the surface 6−8 times with different starting configurations. Figure 2 shows the plot of frictional force versus normal load for $-CH_3$-terminated C_7CH_3, $C_{11}CH_3$, and $C_{14}CH_3$ SAMs. Frictional force is larger for short-chain than for long-chain monolayers under the same normal load. Frictional force changes slowly under lower normal loads but increases dramatically under higher loads, especially under loads larger than 0.6 nN for C_7CH_3. As shown in Figure 3, the tip floats over SAMs under lower loads, then contacts the

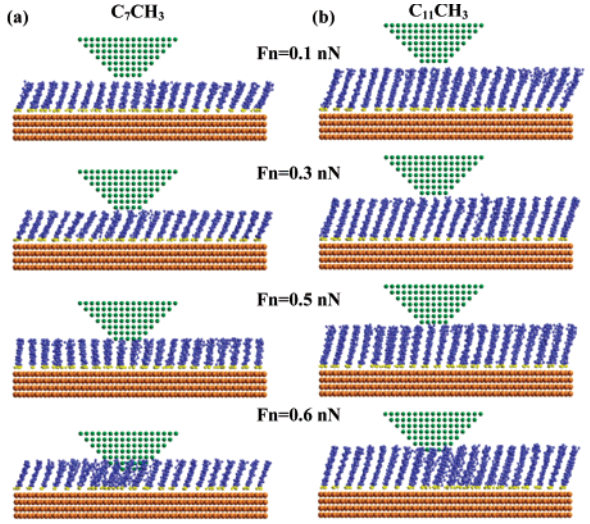

Figure 3. Snapshots of (a) C_7CH_3 and (b) $C_{11}CH_3$ SAMs under different normal loads at 300 K.

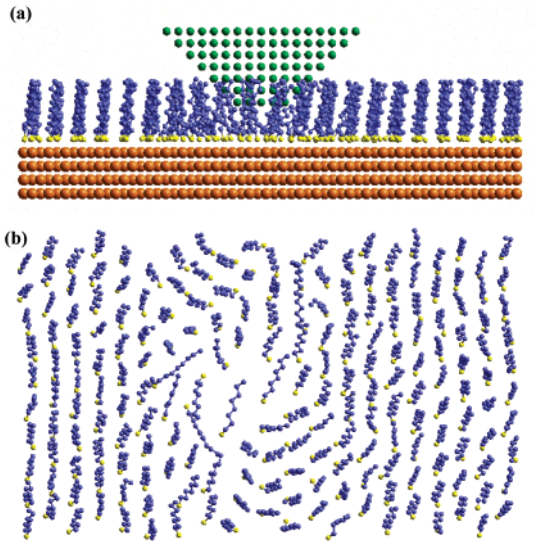

Figure 4. (a) Side and (b) top views of the final configuration for C_7CH_3 SAMs under a high normal load of 1.2 nN (1.6 GPa) at 300 K. The tip is removed from (b) for clarity.

SAMs as load increases, and finally penetrates into the monolayers under very high loads. At a load of 0.5 nN, the tip begins to penetrate into C_7CH_3 monolayer while the tip only contacts $C_{11}CH_3$ monolayer, indicating that the stiffness and shear modulus (along the scan direction) of $C_{11}CH_3$ SAMs are larger than those of C_7CH_3 SAMs due to the compact packing of longer chains. Similar results were found in our previous studies[38] at low temperature. We performed one additional hybrid simulation at an extremely high load of 1.2 nN (equivalent to 1.6 GPa) for C_7CH_3 SAMs. Friction coefficient under this condition is about 20 times larger than that at a load of 0.3 nN. Obviously, large friction is caused by the tip penetration into SAMs. As shown in Figure 4, under this high load, the tip penetrates into SAMs by about 4 Å (side view) and the SAM chains near the tip are pushed to all directions (top view). The chain-length dependence of friction found in this work is consistent with those from AFM/FFM experiments[5−7] at 300 K and from our previous hybrid simulations at 0.1 K.[38] For −OH-terminated SAMs, similar chain-length dependence was also found (Figure 5).

3.2. Terminal Groups. Frictional force is dependent on not only the chain length but also the terminal group

(46) Jorgenson, M. L.; Briggs, J. M.; Contreas, M. L. *J. Phys. Chem.* **1990**, *94*, 1683.
(47) *Cerius² version 4.2 MatSci*; Molecular Simulations Inc.: San Diego, CA, 2000.

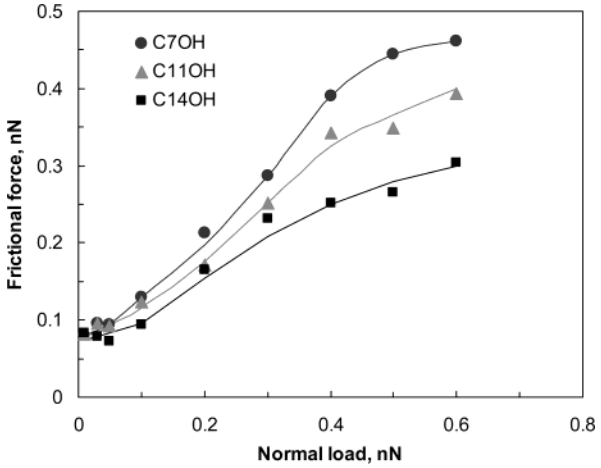

Figure 5. Frictional force vs normal load for −OH-terminated alkanethiol SAMs of different chain lengths at $v = 400$ nm/s, $T = 300$ K, and $\theta = 0°$. Lines are drawn to guide the eyes.

of SAMs. Simulation results in Figures 2 and 5 show that frictional force for −OH-terminated SAMs is much larger than that for $-CH_3$-terminated SAMs under the same load. Similar chain-length dependence is obtained for both $-CH_3$- and −OH-terminated SAMs. However, the trend of the plots is different. For $-CH_3$-terminated SAMs, the increase of frictional force is slower under lower loads and faster at higher loads. For −OH-terminated SAMs, the increase of frictional force is faster at lower loads than at higher loads. For −OH-terminated SAMs, there is a network of hydrogen bonds formed.[35] This hydrogen bond network makes −OH-terminated SAMs stiffer and hard to penetrate by the tip.

The radius of the tip used in simulations was estimated to be ∼3 nm, while it is ∼50 nm in AFM/FFM experiments. It is expected that the tip is easier to penetrate SAMs in simulations than in experiments at the same normal load. However, pressure (i.e., normal load over tip contact area) is in a similar range for tip penetration in both simulations and experiments. In addition, frictional coefficients from simulations and AFM/FFM experiments are compared in this work instead of frictional forces. To obtain friction coefficients, simulated frictional forces were linearly fitted in the range of normal loads before the tip penetrated into SAMs. The slope of the linear line is friction coefficient. Results are shown in Figure 6. As can be seen, friction coefficients for −OH-terminated SAMs are larger than those for $-CH_3$-terminated SAMs for each chain length. For example, the friction coefficient of −OH-terminated SAMs is 0.774 for C_7OH SAMs while it becomes 0.193 for C_7CH_3 SAMs. Similarly, friction coefficient decreases by a factor of 5 for a chain length of C_{12} when the SAM terminal group changes from −OH to $-CH_3$, i.e., from $C_{11}OH$ (0.657) to $C_{11}CH_3$ (0.132). For hydrophobic SAMs, friction coefficients from our previous AFM/FFM experimental measurements[5] are 0.15 and 0.08 for C_7CH_3 and $C_{11}CH_3$ SAMs, respectively. Frictional coefficients are 0.193 and 0.132 from simulations for these two $-CH_3$-terminated SAMs. For −OH-terminated SAMs, there is no experimental data measured under dry conditions, except for one study by Porter and co-workers,[22] in which a friction coefficient of 0.70 for $C_{16}OH$−SAMs/Au(111) was obtained under an atmosphere of flowing argon at room temperature. For other hydrophilic SAMs (e.g., −COOH-terminated SAMs[17]), experiments show the chain-length dependence of friction in ethanol. Our simulation study shows a similar chain-length dependence of friction, i.e., frictional force increases as chain length decreases.

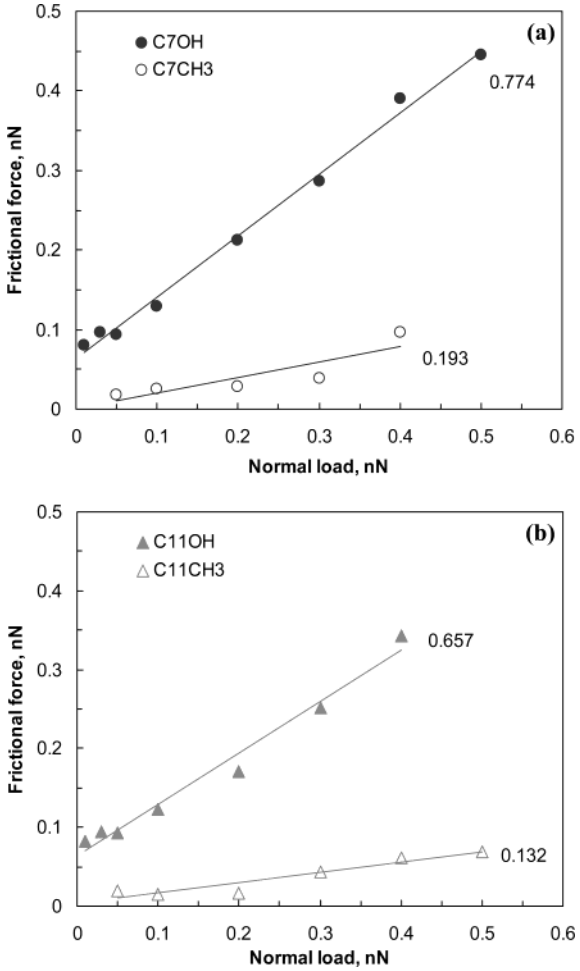

Figure 6. Frictional force vs normal load for (a) C_7OH and C_7CH_3 SAMs and (b) $C_{11}OH$ and $C_{11}CH_3$ SAMs at $v = 400$ nm/s, $T = 300$ K, and $\theta = 0°$. Friction coefficients given in the plots were determined by linearly fitting simulation data.

3.3. Scan Direction. Anisotropy in friction on some monolayers[10−12] and crystals[31,48,49] with respect to different sliding directions has been studied. For alkanethiols/Au(111), the reported friction from AFM/FFM experiments[5−7,20] is often averaged over several forward/backward scans along different directions. Thus, it is hard to know exactly if there is friction anisotropy for this system. Few theoretical studies have been attempted to study friction anisotropy. We expect that frictional force is anisotropic when a tip scans over alkanethiol SAMs since they have a specific tilt direction, represented by the collective azimuthal angle defined as the average angle between the projected vector of the molecular axis on the $x-y$ plane and the $+x$ axis. As shown in Figure 7, the azimuthal angle is ∼30° for $C_{11}CH_3$ SAMs at 300 K, i.e., along the nearest-neighbor (NN) direction. In this work, we carried out hybrid simulations of $C_{11}CH_3$ SAMs at a normal load of 0.5 nN, at which the AFM/FFM tip scanned over the monolayers in different directions. The scan direction is defined by the angle θ between the tip moving direction and the chain tilt direction. Thus, the tip scans along the chain tilt direction if $\theta = 0°$, against the chain tilt direction if $\theta = 180°$, and perpendicular to the chain tilt direction if $\theta = 90°$ or $\theta = 270°$. Figure 8 gives frictional force as a function of scan direction θ from hybrid

(48) Kerssemmakers, J.; De Hossen, J. T. M. *Appl. Phys. Lett.* **1995**, *67*, 347.
(49) Bluhm, H.; Schwarz, U. D.; Wiesendanger, R. *Phys. Rev. B* **1998**, *57*, 161.

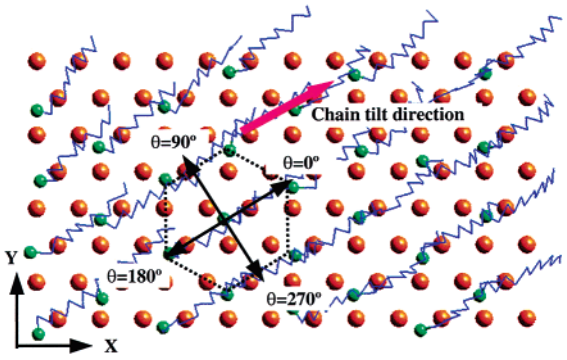

Figure 7. Schematic illustration of the chain tilt and scan directions on alkanethiol SAMs/Au(111) in hybrid molecular simulations. θ is the angle between the tip moving direction and the chain tilt direction. The larger balls represent substrate Au atoms, smaller balls sulfur atoms in molecular chains, and zigzag lines molecular chains.

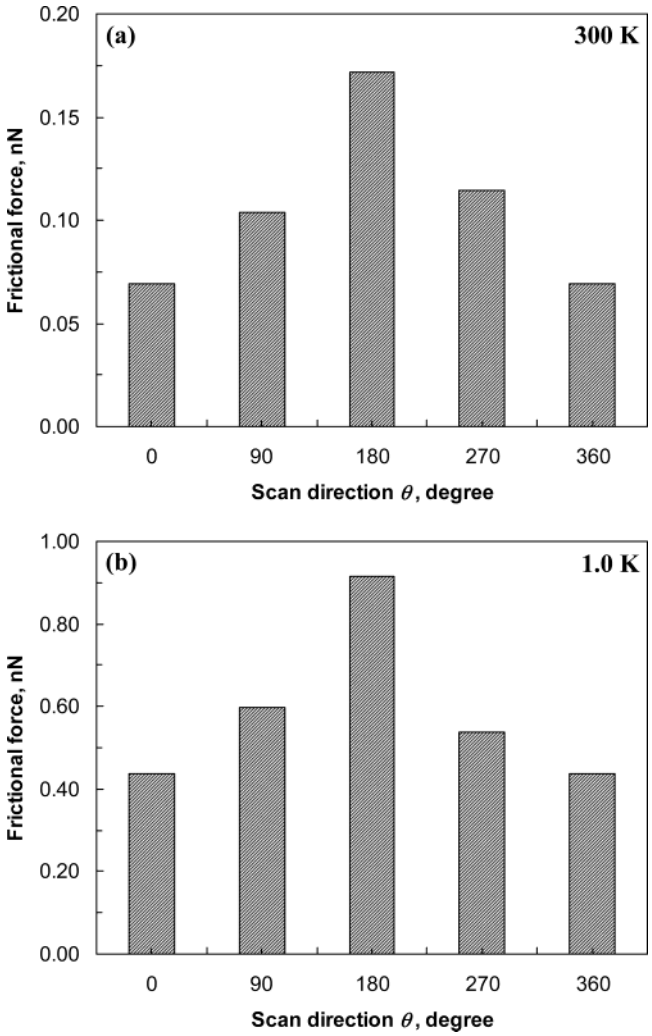

Figure 8. Frictional force as a function of scan direction from hybrid simulations for $C_{11}CH_3$ SAMs on Au(111) at (a) 300 K and (b) 1.0 K. Frictional force is the smallest when scanned along the tilt direction, the largest when scanned against the tilt direction, and between when scanned perpendicular to the tilt direction at both temperatures.

simulations. Results show that friction is the smallest when scanned along the tilt direction ($\theta = 0°$), the largest when scanned against the tilt direction ($\theta = 180°$), and between when scanned perpendicular to the tilt direction ($\theta = 90°$ or $\theta = 270°$). Frictional force is doubled when scan direction is changed from along-the-tilt to against-the-tilt directions for $C_{11}CH_3$ SAMs at 300 K. We also performed hybrid simulations to study friction anisotropy at low temperature (e.g., 1.0 K). Results are presented in Figure 8b. The azimuthal angle is 0° for $C_{11}CH_3$ SAMs at 1.0 K, i.e., closer to the next-nearest-neighbor (NNN) direction. Molecular tilt direction shifts from 0 to 30° when temperature increases from 1.0 to 300 K. As can be seen from Figure 8, the behavior of friction anisotropy is very similar despite different molecular tilt directions at low and high temperatures. Unlike recent simulation results by Ohzono and Fujihira,[12] friction anisotropy for alkanethiol SAMs/Au(111) was observed at low and high temperatures in this work.

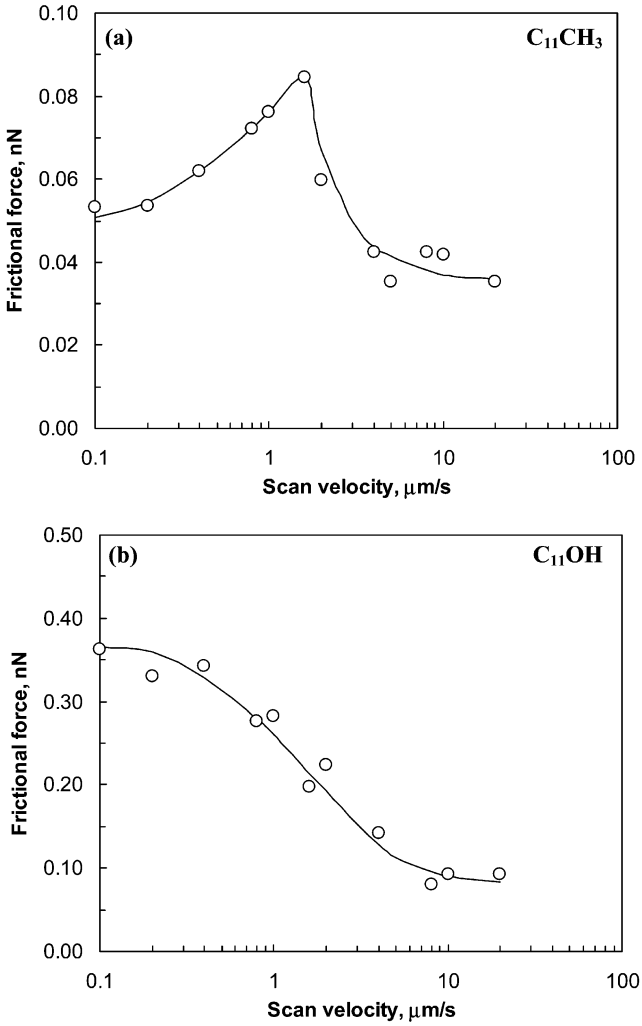

Figure 9. Frictional force as a function of scan velocity for (a) $C_{11}CH_3$ and (b) $C_{11}OH$ SAMs at 300 K. Lines are drawn to guide the eyes.

3.4. Scan Velocity. Several groups have reported the dependence of friction on the scan velocity of the AFM/FFM tip for various systems.[13−17] van der Vegte et al.[15] and Liu et al.[16] reported variations in friction with scan velocity for the monolayers of unsymmetrical *n*-dialkyl sulfides and dialkylammonium salts, respectively. In this work, we performed hybrid simulations of −OH and $-CH_3$ SAMs at scan velocities in the range of 100 nm/s−20 μm/s. As shown in Figure 9a,b, the dependence of frictional force on scan velocity is different for both systems. For $-CH_3$-terminated SAMs, frictional force exhibits a maximum and then approaches a constant value at higher scan velocities. A similar dependence of friction on scan velocity was found in AFM/FFM experiments using a standard tip for hydrophobic $-CH_3$-terminated SAMs[16] and in CFM

experiments with both tip and surface covered by monolayers terminated with $-CH_3$ groups.[15] It was suggested[16] that there is a correlation between existence of the peak and chain melting. For −OH-terminated SAMs, frictional force is almost constant at lower scan velocities, decreases as scan velocity increases, and approaches a constant value at higher scan velocities as shown in Figure 9b. However, AFM/FMM experiments[16] showed the increase of frictional force for hydrophilic −OH-terminated monolayers as scan velocity increases. It should be pointed out that our simulations were performed under dry condition while AFM/FFM experiments were carried out in air under the humidity between 20 and 30%. It is expected that adsorbed water molecules will play an important role in frictional behavior for hydrophilic −OH-terminated surfaces. Thus, it is speculated that the amount of surface water molecules is responsible for the difference in the velocity dependence of friction for −OH-terminated surfaces.

4. Conclusions

In this work, we applied the hybrid simulation technique to study how the frictional properties of alkanethiol SAMs on Au(111) vary with such parameters as chain length, terminal groups, scan direction, and scan velocity at room temperature at the AFM/FFM experimental time scale. Previously, we developed the hybrid simulation technique and applied it to study the chain-length dependence of friction for $-CH_3$-terminated SAMs at low temperature (0.1 K). The main findings from this work are summarized below.

Frictional force decreases with an increase of chain length for both $-CH_3$- and −OH-terminated SAMs. Hydrophilic −OH-terminated SAMs have higher frictional force than hydrophobic $-CH_3$-terminated SAMs. Frictional force as a function of normal load exhibits different behaviors for $-CH_3$- and −OH-terminated SAMs. For $-CH_3$-terminated SAMs, the increase of frictional force is slower under lower loads and faster at higher loads. For −OH-terminated SAMs, the increase of frictional force is faster at lower loads than at higher loads. The hydrogen bond network formed for −OH-terminated SAMs makes them stiffer and hard to penetrate by the tip. These results are in good in agreement with those from AFM/FMM and CFM experiments and from previous simulations.

Unlike recent molecular dynamics simulation results, friction anisotropy for alkanethiol SAMs/Au(111) was observed at both low and high temperatures in this work. The behavior of friction anisotropy is very similar despite different molecular tilt directions at both temperatures. Frictional force is the smallest when scanned along the tilt direction, the largest when scanned against the tilt direction, and between when scanned perpendicular to the tilt direction.

The dependence of frictional force on scan velocity is different for both systems. For $-CH_3$-terminated SAMs, frictional force exhibits a maximum and then approaches to a constant value at higher scan velocities. A similar dependence of friction on scan velocity was found in AFM/FFM and CFM experiments. For −OH-terminated SAMs, frictional force is almost constant at lower scan velocities, decreases as scan velocity increases, and approaches a constant value at higher scan velocities. However, AFM/FMM experiments showed the increase of frictional force for hydrophilic −OH-terminated monolayers as scan velocity increases. It is speculated that the amount of surface water molecules is responsible for the difference in the velocity dependence of friction for −OH-terminated surfaces.

Acknowledgment. The authors thank the National Science Foundation (Grants CMS-9988745, CTS0092699, and CMS-0302139) for financial support.

LA034007G